Properties of Hall magnetohydrodynamic waves modified by electron inertia and finite Larmor radius effects

P. A. Damiano,[1,a)] A. N. Wright,[1] and J. F. McKenzie[2]
[1]*Mathematical Institute, University of St. Andrews, St. Andrews, Fife KY169SS, United Kingdom*
[2]*Astrophysics and Cosmology Research Unit, School of Mathematical Sciences, University of KwaZulu-Natal, Durban 4000, South Africa and Department of Physics, CSPAR, University of Alabama, Hunstville, Alabama 35899, USA*

(Received 19 March 2009; accepted 5 May 2009; published online 3 June 2009)

The linear wave equation (sixth order in space and time) and the corresponding dispersion relation is derived for Hall magnetohydrodynamic (MHD) waves including electron inertial and finite Larmor radius effects together with several limiting cases for a homogeneous plasma. We contrast these limits with the solution of the full dispersion relation in terms of wave normal $(k_\perp, k_\parallel)$ diagrams to clearly illustrate the range of applicability of the individual approximations. We analyze the solutions in terms of all three MHD wave modes (fast, slow, and Alfvén), with particular attention given to how the Alfvén branch (including the cold ideal field line resonance (FLR) [D. J. Southwood, Planet. Space Sci. **22**, 483 (1974)]) is modified by the Hall term and electron inertial and finite Larmor radius effects. The inclusion of these terms breaks the degeneracy of the Alfvén branch in the cold plasma limit and displaces the asymptote position for the FLR to a line defined by the electron thermal speed rather than the Alfvén speed. For a driven system, the break in this degeneracy implies that a resonance would form at one field line for small $k_\perp$ and then shift to another as $k_\perp \to \infty$. However for very large $\omega k_\perp / V_A$, Hall term effects lead to a coupling to the whistler mode, which would then transport energy away from the resonant layer. The inclusion of the Hall term also significantly effects the characteristics of the slow mode. This analysis reveals an interesting "swapping" of the perpendicular root behavior between the slow and Alfvén branches.
 [DOI: 10.1063/1.3142479]

I. INTRODUCTION

The linear theory of magnetohydrodynamic (MHD) waves has been well established. Recently, Ref. 1 provided a very lucid summary and analysis of the linear dispersion relation including thermal, Hall, and electron inertial effects on the Alfvén, fast magnetoacoustic, and slow magnetoacoustic modes. Here we use the Lighthill variables to derive the (sixth order) wave equation for the parallel current and magnetic field perturbations. The associated dispersion relation, also considered by Cramer, is revisited from the point of view of wave normal diagrams $(k_\perp, k_\parallel)$, which provides additional insight into the analysis of the properties of these waves including the characterization of critical layers and reflection points. We also examine different limits with emphasis on how Hall effects modify the inertial Alfvén wave,[2] kinetic Alfvén wave,[3] and the cold ideal MHD field line resonance (FLR).[4] These asymptotic solutions are contrasted with the full dispersion relation to clarify the range of applicability of the individual approximations. Thus we build on the interpretations established by previous authors. Although the paper has a slight emphasis on magnetospheric phenomena, the analysis is completely general and is therefore of interest to those studying "generalized" MHD waves in solar, astrophysical, and tokamak plasmas.

The rest of the paper is broken up into three sections. Section II summarizes the derivation of the wave equation including electron inertia and Hall term effects. Section III presents the full dispersion relation and derives and contrasts several limiting cases against this full solution. Section IV illustrates how the nonrelativistic whistler mode follows from the formulation using "electron MHD." Section V provides a concluding discussion whilst the Appendix summarizes the details of the derivation of the wave equations using Lighthill variables.

II. THE WAVE EQUATIONS FOR INCLUDING THE EFFECTS OF HALL CURRENTS AND ELECTRON INERTIA

The basic equations are those of fluid dynamics expressing conservation of mass, momentum, and energy, coupled with Maxwell's equations for the electromagnetic field. On linearization about a uniform background state (suffix 0), the equations take the form:

$$\frac{\partial \rho}{\partial t} + \rho_0 \nabla \cdot \mathbf{u} = 0, \tag{1}$$

$$\frac{\partial \mathbf{u}}{\partial t} = -\frac{1}{\rho_0} \nabla \left(\frac{B_0 B_z}{\mu_0} + p \right) + \frac{B_0}{\mu_0 \rho_0} \frac{\partial \mathbf{B}}{\partial z}, \tag{2}$$

$$\frac{\partial p}{\partial t} = c^2 \frac{\partial \rho}{\partial t} = -\rho_0 c^2 \nabla \cdot \mathbf{u}, \tag{3}$$

[a)]Now at Thayer School of Engineering, Dartmouth College, Hanover, NH 03755.

$$\frac{\partial \mathbf{B}}{\partial t} = -\nabla \times \mathbf{E}, \tag{4}$$

$$\mathbf{E} = -\mathbf{u}_e \times \mathbf{B}_0 - \frac{\nabla p_e}{en_e} + \mu_0 \lambda_e^2 \frac{\partial \mathbf{j}}{\partial t}, \tag{5}$$

$$\mu_0 \mathbf{j} = \nabla \times \mathbf{B}, \tag{6}$$

$$\mathbf{u}_e = \mathbf{u} - \frac{\mathbf{j}}{en}, \tag{7}$$

in which

$$c = \sqrt{\gamma p_0/\rho_0} \quad \text{(speed of sound)}, \tag{8}$$

$$\lambda_e^2 = \frac{v_{A_e}^2}{\Omega_e^2} = \frac{v_A^2}{\Omega_e \Omega_p} \quad \text{(“electron skin depth”)}, \tag{9}$$

$$v_A = \frac{B_0}{\sqrt{\mu_0 \rho_0}} \quad \text{(Alfvén speed based on protons)}, \tag{10}$$

$$v_{Ae}^2 = \frac{B_0^2}{\mu_0 m_e n_0} \quad \text{(square of Alfvén speed based on electrons)}, \tag{11}$$

$$\Omega_{p,e} = eB_0/m_{p,e} \quad \text{(cyclotron frequency)}.$$

In the momentum Eq. (2) the $\mathbf{j} \times \mathbf{B}_0$ force has been replaced by the magnetic pressure and tension terms using Ampère's law (6), in which we neglected the displacement current, which is valid in our charge neutral approximation for frequencies ω much less that the electron plasma frequency $\omega_{p,e}$. The background magnetic field $\mathbf{B}_0$ is aligned with the z-axis. In the dissipationless (“collisionless”) case it is convenient to replace the energy equations with the adiabatic condition (3). The electric field is given by Ohm's law [Eq. (5)], which includes Hall current effects, through the relation (7) between the electron velocity $\mathbf{u}_e$, the bulk (proton) velocity $\mathbf{u}$, and the current $\mathbf{j}$, and also electron inertia through the third term on the right hand side of Eq. (5), which is essentially the electron equation of motion.

Standard operations (see Appendix) yield the following two coupled wave equations for the parallel current $j_\parallel$:

$$\mathcal{L}_A j_\parallel = \frac{v_A^2}{\mu_0 \Omega_p} \frac{\partial}{\partial z} \nabla^2 \frac{\partial B_z}{\partial t},$$

$$\mathcal{L}_A \equiv \frac{\partial^2}{\partial t^2}(1 - \lambda_e^2 \nabla^2) - v_A^2 \frac{\partial^2}{\partial z^2}, \tag{12}$$

and the parallel magnetic field B_z,

$$\mathcal{L}_{MA} B_z = -\frac{\mu_0 v_A^2}{\Omega_p} \frac{\partial}{\partial z}\left(\frac{\partial^2}{\partial t^2} - c^2 \nabla^2\right) \frac{\partial j_\parallel}{\partial t},$$

$$\mathcal{L}_{MA} \equiv \left(\frac{\partial^2}{\partial t^2} - c^2 \nabla^2\right) \frac{\partial^2}{\partial t^2}(1 - \lambda_e^2 \nabla^2) - v_A^2 \nabla^2 \left(\frac{\partial^2}{\partial t^2} - c^2 \frac{\partial^2}{\partial z^2}\right). \tag{13}$$

Hence the wave equation for B_z (or $j_\parallel$) is

$$\mathcal{L}_A \mathcal{L}_{MA}(B_z, j_\parallel) = -\left(\frac{v_A^2}{\Omega_p}\right)^2 \frac{\partial^2}{\partial z^2} \nabla^2 \left(\frac{\partial^2}{\partial t^2} - c^2 \nabla^2\right) \frac{\partial^2}{\partial t^2}(B_z, j_\parallel). \tag{14}$$

This sixth order (in time and space) wave equation displays how the standard MHD waves, as represented by the Alfvén operator $\mathcal{L}_A$, modified by electron inertia, and the magnetoacoustic operator $\mathcal{L}_{MA}$, also so modified, are coupled through the Hall current terms on the right hand side of Eq. (13). The wave system is anisotropic by virtue of the preferred direction $\hat{z}(\mathbf{B}_0)$ and dispersive through electron inertia and Hall current effects that introduce the cyclotron frequency. The anisotropic and dispersive properties of the wave system are analyzed in Sec. III in terms of the dispersion equation given by the Fourier image of Eq. (14) in $(\omega, \mathbf{k})$ space.

III. PROPAGATION PROPERTIES: WAVE NORMAL DIAGRAMS

For plane wave disturbances varying as $\exp i(\omega t - \mathbf{k} \cdot \mathbf{r})$, the Fourier image of the wave Eq. (14) yields the dispersion equation (see also Ref. 1)

$$[\omega^2(1 + \lambda_e^2 k^2) - v_A^2 k_z^2][\omega^2(1 + \lambda_e^2 k^2)(\omega^2 - c^2 k^2) - v_A^2 k^2(\omega^2 - c^2 k_z^2)] = \left(\frac{v_A^2 \omega}{\Omega_p}\right)^2 k^2 k_z^2 (\omega^2 - c^2 k^2). \tag{15}$$

Its structure demonstrates how the Alfvén mode (in MHD defined by the zero of the first square bracket on the left hand side) and the magnetoacoustic modes (given by the zero of the second square bracket) are modified by the coupling introduced by Hall current effects represented by the right hand side of Eq. (15). A number of special cases illustrate how the coupling works. For the direct numerical solution of Eq. (15), we use the algorithm outlined in Ref. 5 (p. 179) for the solution of cubic equations.

A. Single fluid MHD limit, $\lambda_e = 0$, $\omega/\Omega_p = 0$, $c \neq 0$

In the single fluid MHD limit, Eq. (15) reduces to

$$[\omega^2 - v_A^2 k_z^2][\omega^2(\omega^2 - c^2 k^2) - v_A^2 k^2(\omega^2 - c^2 k_z^2)] = 0, \tag{16}$$

in which the zero of the first bracket on the left hand side yields the Alfvén mode planes $k_z = \pm \omega / v_A$. The zero of the second bracket yields the fast and slow magnetoacoustic modes. The wave normal (or $\mathbf{k}$) diagrams (normalized by ω / V_A) are displayed in Fig. 1 for the case $c^2/v_A^2 = 0.5$. The

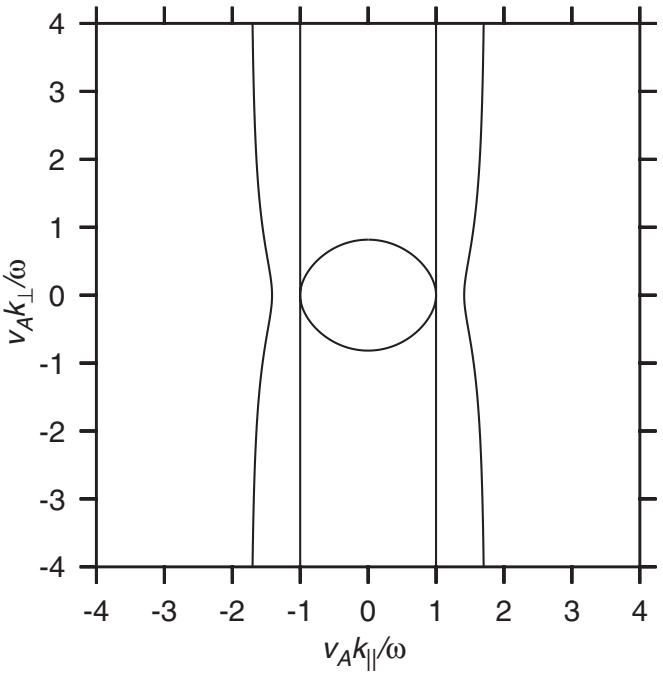

FIG. 1. Plot of $k_\perp$ vs $k_\parallel$ [from Eq. (16)] normalized by ω/v_A showing the MHD modes ($\lambda_e=0$, $\omega/\Omega_p=0$) for $c^2/v_A^2=0.5$. The slow mode cuts the normalized $k_\parallel$ axis at $v_A k_\parallel/\omega=\pm v_A/c=\pm\sqrt{2}$, while the fast mode cuts the $k_\perp$ axis at $v_A k_\perp/\omega=\pm 1/\sqrt{c^2/v_A^2+1}=\pm\sqrt{2/3}$.

fast mode is the oblate spheroid, which cuts the normalized $k_\perp$ axis at $v_A k_\perp/\omega=\pm 1/\sqrt{c^2/v_A^2+1}$, while the slow mode cuts the normalized $k_\parallel$ axis at $v_A k_\parallel/\omega=v_A/c$, representing an indentation from the planes $k_z=\pm\omega^2\sqrt{1/c^2+1/v^2}$.

B. Cold plasma ($c=0$), $\lambda_e=0$, with Hall current $\omega/\Omega_p\neq 0$

In this case Eq. (15) reduces to

$$\left(\frac{\omega^2}{v_A^2}-k_z^2\right)\left(\frac{\omega^2}{v_A^2}-k^2\right)=\left(\frac{\omega}{\Omega_p}\right)^2 k^2 k_z^2, \tag{17}$$

which on noting that $k^2=k_\perp^2+k_z^2$ may be rearranged to give

$$k_\perp^2=\frac{\left(k_z^2-\dfrac{\omega^2/V_A^2}{1-\omega/\Omega_p}\right)\left(k_z^2-\dfrac{\omega^2/V_A^2}{1+\omega/\Omega_p}\right)}{\left(\dfrac{\omega^2/V_A^2}{(1-(\omega/\Omega_p)^2)}-k_z^2\right)}.$$

The solutions are plotted in Fig. 2. Thus the fast mode sphere $k^2=\omega^2/v_A^2$ is distorted by Hall current effects to an oblate spheroid, which intersects the k_z axis at $(\omega/v_A)/\sqrt{1+\omega/\Omega_p}$, and the Alfvén mode plane $k_z=\omega/v_A$ develops a bump which intersects the parallel axis at $k_z=(\omega/v_A)/\sqrt{1-\omega/\Omega_p}$, and the asymptote ($k_\perp\to\infty$) is displaced to $k_z=(\omega/v_A)/\sqrt{1-(\omega/\Omega_p)^2}$. These characteristics are evident in Fig. 2 where we plotted the solution of Eq. (17) for the $\omega/\Omega_p=0$ (panel a represents the absence of Hall effects) and $\omega/\Omega_p=0.9$ (panel b). The slow mode **k** diagram is displaced to infinity in the cold plasma limit. In panel b, the distortion of the Alfvén branch implies that waves in a weakly inhomogeneous medium, using JWKB theory, would be reflected

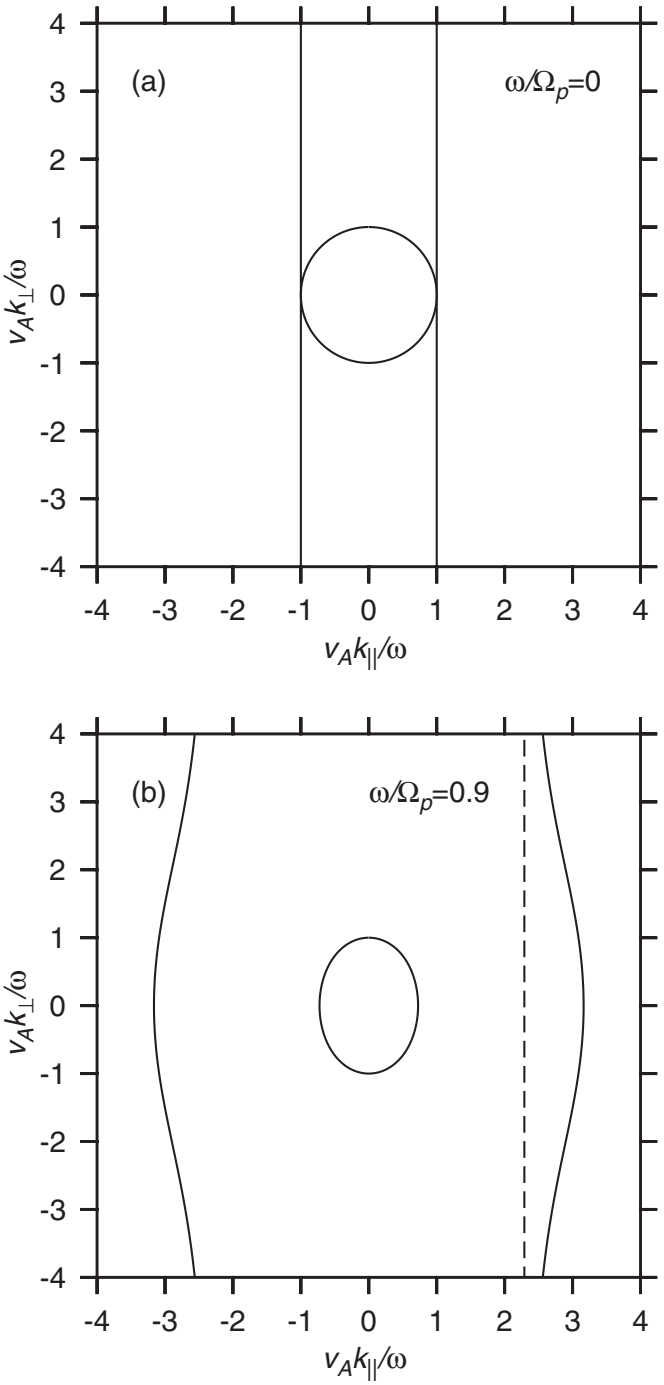

FIG. 2. Plot of $k_\perp$ vs k_z [from Eq. (17)] normalized by ω/v_A with $\lambda_e=0$ ($m_e=0$) for (a) $\omega/\Omega_p=0$ and (b) $\omega/\Omega_p=0.9$. In panel (b) the modified fast mode cuts the normalized $k_\parallel$ axis at $v_A k_z/\omega=1/\sqrt{1+\omega/\Omega_p}=0.725$ while the modified Alfvén mode does the same at $v_A k_z/\omega=1/\sqrt{1-\omega/\Omega_p}=3.16$. The dashed line denotes the asymptotic line for the modified Alfvén mode given by $v_A k_z/\omega=1/\sqrt{1-(\omega/\Omega_p)^2}=2.29$.

at the position defined by the tip of the bump ($k_\perp=0$) and would also pile up at a critical layer as $k_\perp\to\infty$. This modified Alfvén mode is also referred to as the ion cyclotron mode.[1] The critical layer also implies that, due to Hall effects, the position of the classical FLR (Ref. 4) is shifted to this new asymptote. The radius vector **k** from the origin to the curves is the wave normal (or phase) direction and a small arrow drawn normal to the **k** curve would represent the

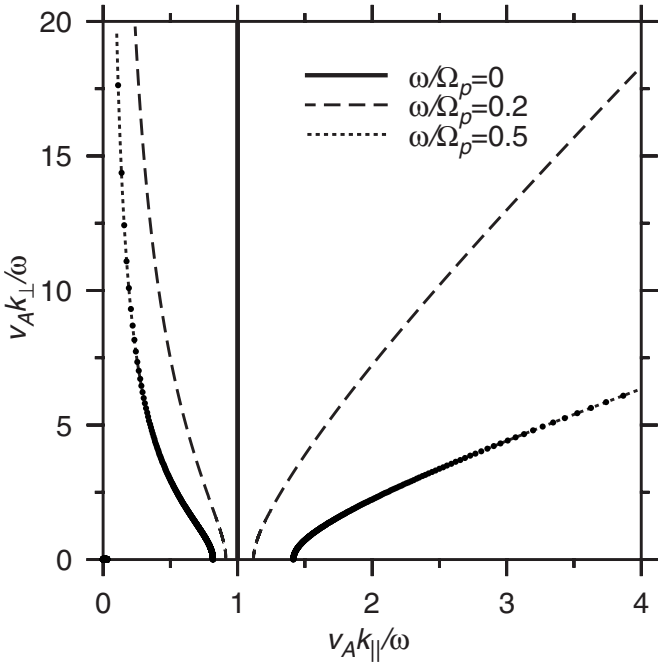

FIG. 3. Plot of $k_\perp$ vs $k_\parallel$ (first quadrant only) normalized by ω/v_A in the incompressible limit ($c\to\infty$) but incorporating the Hall current [Eq. (18a)] for various values of ω/Ω_p. Superimposed on the $\omega/\Omega_p=0.9$ case is the numerical solution of the full dispersion relation [Eq. (15)] for $c^2/v_A^2=1000$.

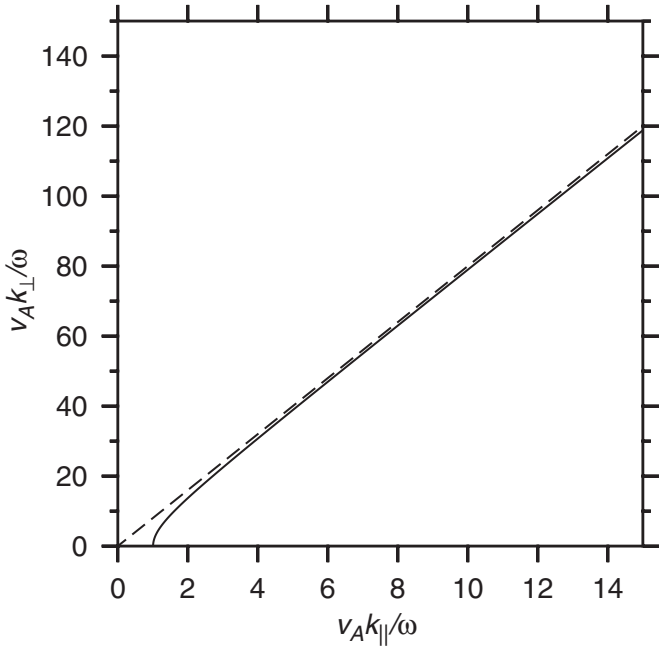

FIG. 4. Alfvén wave branch modified by electron inertial effects (solid line). The resonance cone defined by $\cot^{-1}(\omega/\sqrt{\Omega_e\Omega_p})$ is displayed using the dashed line.

direction of the ray. Note as well how the "Alfvén-ion cyclotron" mode develops a "resonance" as $\omega\to\Omega_p$. Further details on the limit considered in this section can also be found in a lucid discussion in Ref. 1.

C. Incompressible plasma ($ck_z/\omega\to\infty$) with Hall current

In the incompressible limit ($c\to\infty$) and with $\lambda_e=0$, Eq. (15) becomes

$$\left(k_z^2-\frac{\omega^2}{v_A^2}\right)^2=\left(\frac{\omega}{\Omega_p}\right)^2k^2k_z^2, \tag{18a}$$

which, on reverting to polars $\mathbf{k}=k(\sin\theta,\cos\theta)$, yields

$$k^2=\frac{\omega^2/v_A^2}{\cos\theta(\cos\theta\mp\omega/\Omega_p)}. \tag{18b}$$

In this case the Alfvén and slow modes are modified by the Hall terms to give the wave normal diagrams shown in Fig. 3, where we solved Eq. (18a) for several values of ω/Ω_p. The Alfvén and slow branches are degenerate for $\omega/\Omega_p=0$, but as this ratio increases from zero they separate with the slow branch displaced to the right and Alfvén to the left. Note how the minus sign in Eq. (18b) yields a resonant cone at $\cos\theta=\omega/\Omega_p$ (evident for the slow mode), whereas the plus sign gives the asymptote $k_\perp\to\infty$, $k_\parallel\to0$ as $\theta\to\pi/2$ (Alfvén branch). However this latter result is modified by the inclusion of electron inertia terms, which become increasingly important for quasiperpendicular propagation (which is discussed in Sec. III D). The solution of the full dispersion relation [Eq. (15)], solved for $c^2/v_A^2=1000$ and $\omega/\Omega_p=0.9$, is also plotted (dots), showing that Eq. (18a) is an accurate representation of the full dispersion relation for large (but finite) values of c. The full dispersion relation was solved at equal intervals of θ. Sufficient resolution as $\theta\to\pi/2$ required many points for smaller θ, which is characterized by the progression of the dots toward a solid line as $\theta\to0$.

D. Hall current absent $\omega/\Omega_p=0$ but with electron inertia $\lambda_e\neq0$

Strictly speaking this limit is only valid for quasitransverse propagation. With the right hand side zero, Eq. (15) factors into the Alfvén mode (the zero of the first bracket on the left hand side) and the magnetoacoustic modes (the zero of the second bracket) both modified by λ_e. Thus the Alfvén mode becomes

$$k_z^2=\frac{\omega^2}{v_A^2}\frac{(1+\lambda_e^2k_\perp^2)}{(1-\omega^2/\Omega_e\Omega_p)}, \tag{19a}$$

$$\approx\frac{\omega^2}{v_A^2}(1+\lambda_e^2k_\perp^2),\quad \omega\ll\Omega_e\Omega_p, \tag{19b}$$

where we used Eq. (9) for λ_e^2. This is commonly referred to as the inertial Alfvén mode (e.g., Ref. 2), which permits energy propagation across the magnetic field lines. The wave normal diagram defined by Eq. (19b) is shown in Fig. 4, illustrating a resonance cone at the wave normal angle, $\cot^{-1}(\omega/\sqrt{\Omega_e\Omega_p})$. The perpendicular group velocity attains a maximum $(\omega/\sqrt{2\Omega_e\Omega_p}v_A$ at $\cot^{-1}\omega/\sqrt{3/\Omega_e\Omega_p})$. Although this is a rather small fraction of the Alfvén speed, it is important since it removes the resonant singularity associated with a purely MHD resonance (e.g., see Ref. 6) by dispersing energy away from the ideal resonant field line. In Fig. 4, we expressed λ_e in terms of m_e/m_p and ω/Ω_p for consistency

with the rest of the plots. Values of $m_e/m_p=1/16$ and $\omega/\Omega_p=0.5$ were chosen to make the resonance cone structure clear. This does not contradict the choice of $\omega/\Omega_p=0$ for this section, but simply defines a value for λ_e. The magnetoacoustic modes given by the zero of the second bracket of Eq. (15) are governed by

$$k_\perp^2[v_A^2c^2k_z^2-\omega^2(v_A^2+c^2)]+(\omega^2-k_z^2v_A^2)(\omega^2-k_z^2c^2) = -\omega^2\lambda_e^2k^2(\omega^2-c^2k^2). \quad (20)$$

In the absence of electron inertia (λ_e), the zero left hand side describes the classical MHD wave normal diagram, in which the fast mode is an oblate spheroid of revolution about k_z and the slow mode is the plane $k_z=\omega[(1/c^2)+(1/v_A^2)]^{1/2}$. However if $\lambda_e\neq 0$ this latter mode now exhibits a resonance cone at $\cos\theta=\omega/\sqrt{\Omega_e\Omega_p}$, which shows how the electron mass first appears through the lower hybrid frequency $\sqrt{\Omega_e\Omega_p}$. On the other hand the fast mode is more or less unaffected except for propagation nearly perpendicular to $\mathbf{B}_0$, in which case Eq. (20) approximates to

$$v_{ph_\perp}^2=\left(\frac{\omega}{k_\perp}\right)^2=\frac{v_A^2+c^2(1+\lambda_e^2k^2)}{1+\lambda_e^2k^2}. \quad (21)$$

Thus electron inertial effects modify the phase speed from the MHD fast speed $\sqrt{v_A^2+c^2}$, for $\lambda_e k\ll 1$, to the sound speed c, for $\lambda_e k_\perp\gg 1$. In effect there is a quasiresonance ($k_\perp\to\infty$) as $\omega\to\sqrt{\Omega_e\Omega_p}$ (the lower hybrid frequency) for c small. It is interesting to note that for stationary waves propagating with speed $U(\omega=Uk)$ Eq. (21) shows that $k^2<0$ (evanescent waves) either for $U>\sqrt{v_A^2+c^2}$ or $U<c$. In the former case the inclusion of nonlinear terms (which can bring about a balance between nonlinear wave steepening and dispersion) soliton structures propagating perpendicular to the ambient magnetic field can be realized.[7–9]

E. Cold plasma with Hall current ($\omega/\Omega_p\neq 0$) and electron inertia ($\lambda_e\neq 0$)

In the limit of cold plasma (but incorporating electron inertia), Eq. (15) reduces to

$$[\omega^2(1+\lambda_e^2k^2)-v_A^2k_z^2][\omega^2(1+\lambda_e^2k^2)-v_A^2k^2] = \left(\frac{v_A^2\omega}{\Omega_p}\right)^2k^2k_z^2. \quad (22)$$

Since $c=0$, only the Alfvén and fast modes modified by the Hall current are present. Figure 5(a) displays the wave normal diagram given by Eq. (22) for various values of $\omega/\Omega_p<1$. An artificial value of $m_e/m_p=1/16$ was used to bring out features for relatively small values of $v_Ak_\perp/\omega$ associated with the "isotropic" mode. This diagram is similar to that shown in Fig. 2, the fast mode becomes more oblate and the Alfvén mode develops a bump as Hall effects increase. In this case, the roots for $v_Ak_\parallel/\omega$ are modified to $1/\sqrt{1-(m_e/m_p)(\omega/\Omega_p)^2+\omega/\Omega_p}$ and $1/\sqrt{1-m_e/m_p(\omega/\Omega_p)^2-\omega/\Omega_p}$ for the fast and Alfvén modes,

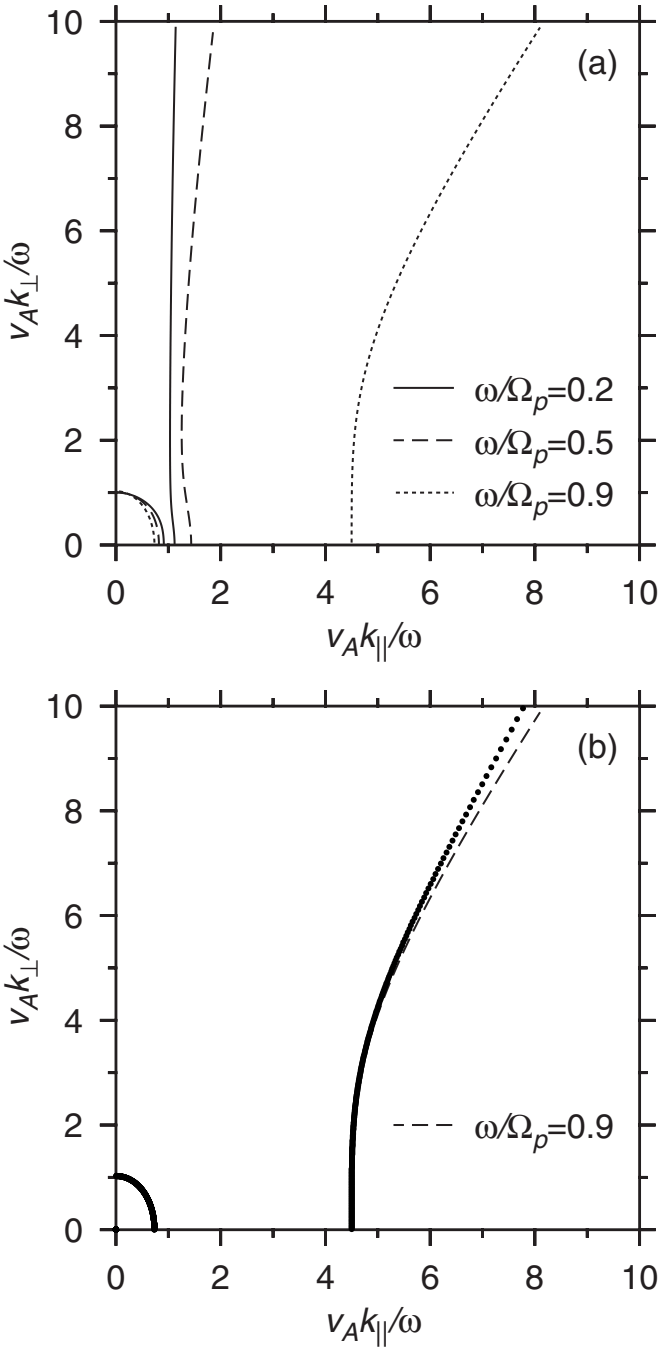

FIG. 5. (a) Plot of $k_\perp$ vs $k_\parallel$ (first quadrant only) normalized by ω/V_A in the cold plasma limit ($c=0$), but incorporating Hall and inertial effects [Eq. (22)]. Several values of $\omega/\Omega_p<1$ are considered. (b) Comparisons of Eq. (22) (dashed line) with the full dispersion relation [Eq. (15)] for $\omega/\Omega_p=0.9$ and $c^2/V_A^2=10^{-4}$. The solution of the full dispersion relation is plotted with dots.

respectively. In the Alfvén case, the root tends to infinity very quickly as ω/Ω_p tends to $(1-(m_e/m_p)(\omega/\Omega_p)^2)$ (which occurs at $\omega/\Omega_p\approx 0.949$). In Fig. 5(b), Eq. (22) is contrasted with the numerical solution of the full dispersion relation for $\omega/\Omega_p=0.9$ and $c^2/v_A^2=10^{-4}$. The solution is very sensitive to small but finite values of $\beta=c^2/v_A^2$ at large perpendicular wave numbers. This difference becomes smaller as the value of β decreases.

Figure 6(a) displays examples for $\omega/\Omega_p>1$. In this case

only the fast mode exists and the perpendicular root is given by $v_A k_\perp/\omega = \pm 1/\sqrt{1-(m_e/m_p)(\omega/\Omega_p)^2}$. For the artificial parameters considered, $k_\perp \to \infty$ when $\omega/\Omega_p \to 4$. This effect is manifested in Fig. 6(a), by the change in topology from a closed curve to the formation of a resonant cone at $\omega/\Omega_p = 4.1$. Figure 6(b) contrasts the solution of Eq. (22) with that of the full dispersion relation [Eq. (15)] for two values of c/V_A. As c/v_A decreases, the resonance cone predicted from Eq. (22) is approached.

F. Modifications introduced to the Alfvén and slow modes by electron inertia, Hall current, and Larmor radius effects

The modifications to the Alfvén mode introduced by the above-mentioned effects have been discussed separately by Ref. 2 for electron inertia and Ref. 3 for finite Larmor radius effects, and in combined form by Refs. 10–12 and 1. In the general dispersion Eq. (15), we make the following assumptions:

(a) $k_\perp \gg k_z \Rightarrow k^2 \to k_\perp^2$, and
(b) $\omega \ll k_\perp c$.

On dividing through by $-\omega^2(v_A^2 k_\perp^2 \omega^2)$, Eq. (15) approximates to

$$\left[1+\lambda_e^2 k_\perp^2 - \frac{v_A^2 k_z^2}{\omega^2}\right]\left[1+\frac{c^2}{v_A^2}\left(1+\lambda_e^2 k_\perp^2 - \frac{v_A^2 k_z^2}{\omega^2}\right)\right] \simeq \frac{v_A^2 k_z^2}{\omega^2}(k_\perp^2 \rho_s^2), \tag{23}$$

in which ρ_s is the thermal Larmor radius defined as

$$\rho_s = c/\Omega_p. \tag{24}$$

Equation (23) may be viewed as a quadratic for $(1+\lambda_e^2 k_\perp^2 - V_A^2 k_z^2/\omega^2)$. If $\beta(\equiv c^2/v_A^2)$ is small, the smaller root approximately gives

$$k_z^2 = \frac{\omega^2}{v_A^2}\left(\frac{1+\lambda_e^2 k_\perp^2}{1+\rho_s^2 k_\perp^2}\right) + 0(\beta), \tag{25}$$

whilst the larger root yields

$$\frac{v_A^2 k_z^2}{\omega^2} \doteq \frac{1+k_\perp^2 \rho_s^2}{c^2/v_A^2}, \tag{26}$$

or

$$k_z^2 = \frac{\omega^2}{c^2}(1+k_\perp^2 \rho_s^2) + 0(\beta).$$

The first root, Eq. (25), is the Alfvén wave plane, modified by inertial and Larmor radius/Hall current effects. The second root, Eq. (26), is the slow mode modified by Larmor radius effects. Note that this modified Alfvén mode displays an asymptote ($k_\perp \to \infty$) at

$$k_z = \frac{\omega}{v_A}\frac{\lambda_e}{\rho_s} = \frac{\omega}{v_{te}}, \tag{27}$$

in which

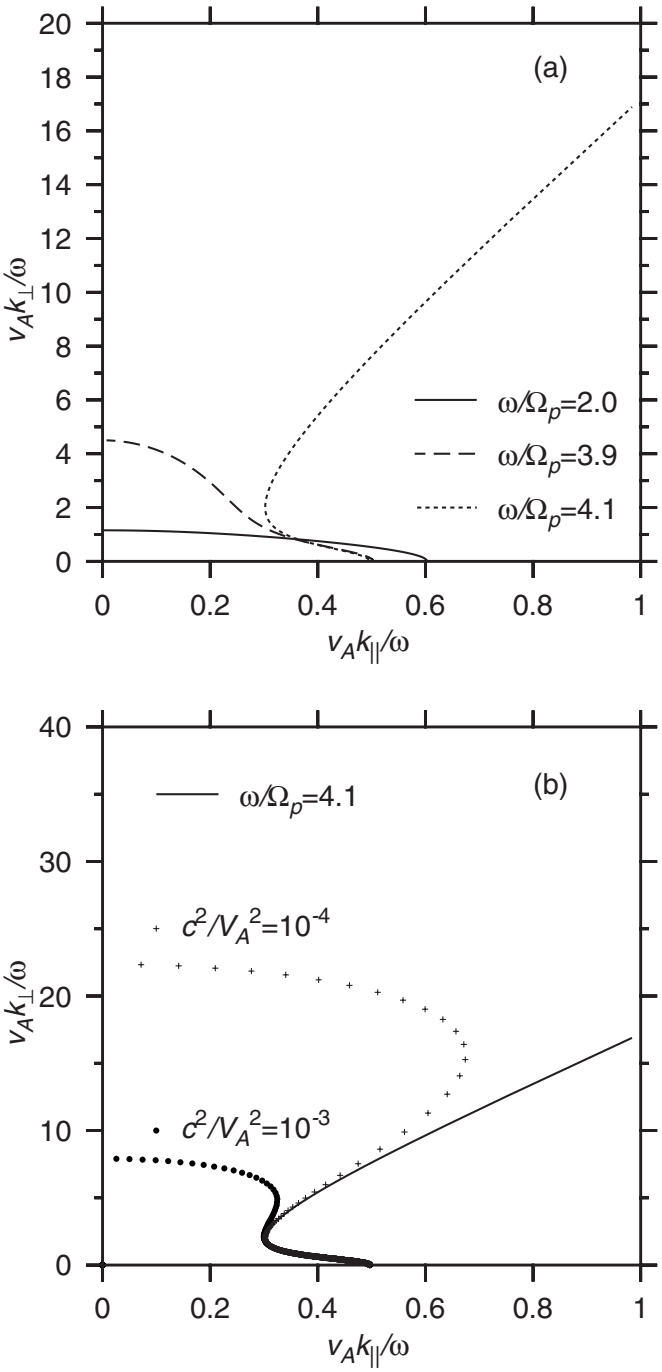

FIG. 6. (a) Same as Fig. 5 except for values of $\omega/\Omega_p > 1$. (b) Comparisons of Eq. (22) with the full dispersion relation [Eq. (15)] for $\omega/\Omega_p = 0.9$ and for values of c^2/V_A^2 of 10^{-4} and 10^{-3}.

$$v_{te} = c\sqrt{\frac{m_p}{m_e}} = \sqrt{(\gamma_e T_e + \gamma_i T_i)k/m_e}.$$

Thus the FLR, associated with $k_\perp \to \infty$ now occurs at a speed defined by an effective temperature and the electron mass rather than the Alfvén speed. Additionally, it is worth noting that although the resonance is at one frequency ω as $k_\perp \to \infty$, this can be very different from the low $k_\perp$ value of the frequency on the same field line. It is likely that if driven at ω_d, a time dependent solution would couple energy to the Alfvén mode on one field line. This could then

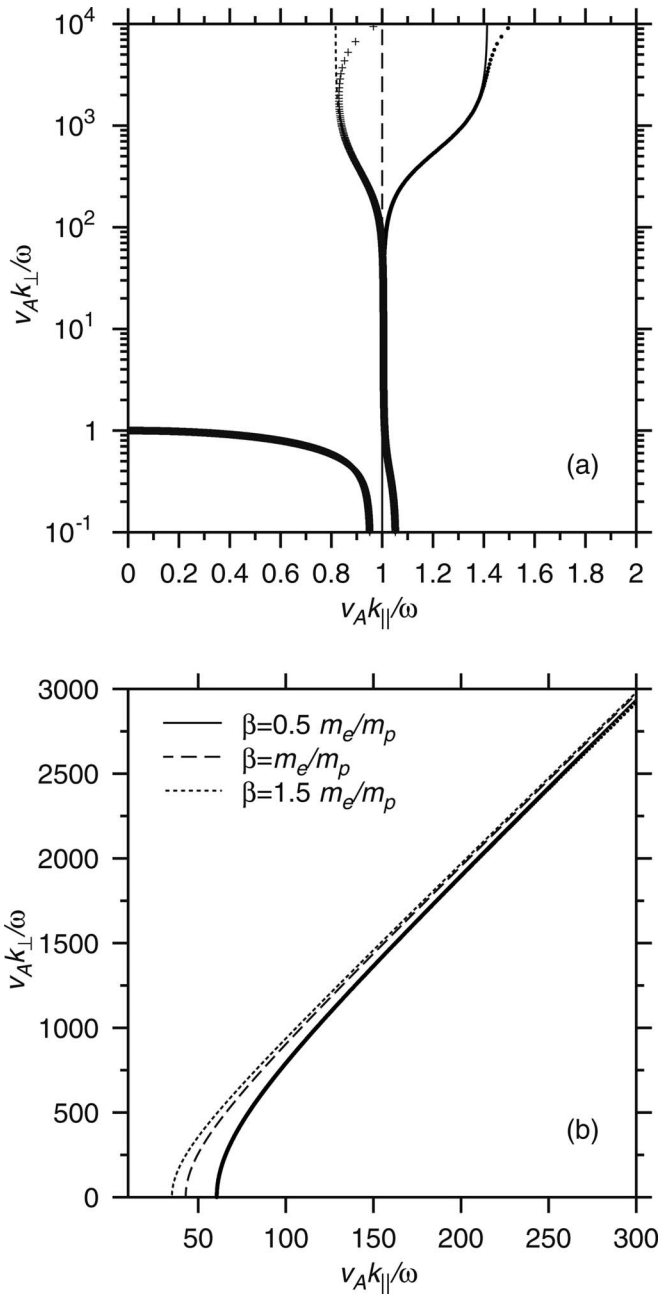

FIG. 7. (a) Plot of Alfvén branch from Eq. (25) for $\omega/\Omega_p=0.1$ and $\beta=0.5m_e/m_p$ (solid line), $\beta=m_e/m_p$ (dashed line), and $\beta=1.5m_e/m_p$ (dotted line). The solution of the full dispersion relation [Eq. (15)] is superimposed for $\beta=0.5m_e/m_p$ (dots) and $\beta=1.5m_e/m_p$ (pluses). This includes the fast mode branch. (b) Plot of slow branch for the same values of ω/Ω_p and β as used in (a). Full dispersion relation comparison is for $\beta=0.5m_e/m_p$ alone.

phase mix (thereby increasing $k_\perp$ and developing $v_{g_\perp}$) and drift to a field line, where $v_{g_\perp}=0$ at which energy would accumulate and correspond to the $k_\perp\to\infty$ asymptote (resonant singularity).

1. $\beta\sim m_e/m_p$

Figure 7(a) displays the Alfvén mode solution of Eq. (25) for $\beta=0.5m_e/m_p$, m_e/m_p, $1.5m_e/m_p$, and $\omega/\Omega_p=0.1$. Since $v_{th}=c\sqrt{m_e/m_p}$, when $v_{th}=V_A$, $\beta=m_e/m_p$. The limit $\beta\ll m_e/m_i$ corresponds to the inertial Alfvén wave limit [numerator of Eq. (25) dominates], while $\beta\gg m_e/m_p$ is the kinetic Alfvén wave limit (denominator dominates). This is evident in Fig. 7(a) by the two branches that emerge at large $k_\perp$, where the solid line denotes the inertial branch and the dotted line the kinetic branch. These are the asymptotes predicted by Eq. (27). When $\lambda_e=\rho_s$, the two limits balance and the ideal single fluid Alfvén relation $\omega=k_z V_A$ is recovered (dashed line).

For intermediate values of $\omega k_\perp/V_A$, resonance cones exist and, therefore, as in the simple electron inertial limit considered in Sec. III D, energy can propagate perpendicular to the ambient magnetic field (in different directions depending on whether $\beta\ll m_e/m_i$ or $\beta\gg m_e/m_i$). As $\omega k_\perp/V_A$ increases further, the resonance cone becomes an asymptote and the energy will be confined to the resonance layer.

Superimposed on the plot is the solution of the full dispersion relation [Eq. (15)] for the two limits $\beta=0.5m_e/m_p$ (dots) and $\beta=1.5m_e/m_p$ (pluses). Both the fast and Alfvén branches are evident here (although the fast mode is similar for both values of β). Hall effects lead to a difference at the Alfvén branch, for small $k_\perp$, from the solution of Eq. (27). This is to be expected since the relation is valid only in the limit $k_\perp\gg k_\parallel$. For large values of $\omega k_\perp/V_A$, there is also a divergence from the solution given by Eq. (25) due to the mode becoming more "whistler" in character, with the end result that the balance between inertial and kinetic effects is destroyed (in the limit of large $\omega k_\perp/V_A$) and instead a whistler resonance cone emerges, which permits propagation of energy across magnetic field lines.

Both the inertial and kinetic Alfvén wave limits yield perpendicular group velocities that point in opposite directions and exactly balance one another when $v_{th}=V_A$. In this case the wave has vanishingly small perpendicular group velocity, which is associated with the singular accumulation of energy through a resonance. In the Earth's magnetosphere, the inertial terms dominate toward the ionospheric boundary while the kinetic terms dominate toward the equatorial region. An interesting consequence of this (as noted by Refs. 11 and 12) is that in the Earth's dipolar magnetic field the ray path of a wave propagating along the field line and bouncing between ionospheric boundaries can follow a 'figure of 8' pattern as it passes through the inertial and kinetic regimes. This gives rise to a "nondispersive" mode in the sense that the perpendicular group velocity averaged over a cycle for the wave is zero. Thus although kinetic and inertial effects do not balance locally, they may do so from a "bounce-averaged" point of view.

The second root Eq. (26) is the slow mode modified by finite Larmor radius/Hall current effects, displays a resonance cone at an angle $\tan^{-1}(\Omega_p/\omega)$, and the finite Larmor radius effect permits the slow mode to propagate energy across the field lines, in a fashion analogous to finite electron inertia effects on the Alfvén mode, with a maximum speed $(\sqrt{2}/3)(\omega/\Omega_p)c$ at an angle $\tan^{-1}(\sqrt{3}\omega/\Omega_p)$. Figure 7(b) displays the solution of Eq. (26) for the same three values of β. The resonance cone is evident (consistent for all three curves since ω/Ω_p is fixed at 0.1) and as β increases the root in $k_\parallel$ (with $k_\perp=0$) is shifted to smaller values (consistent with

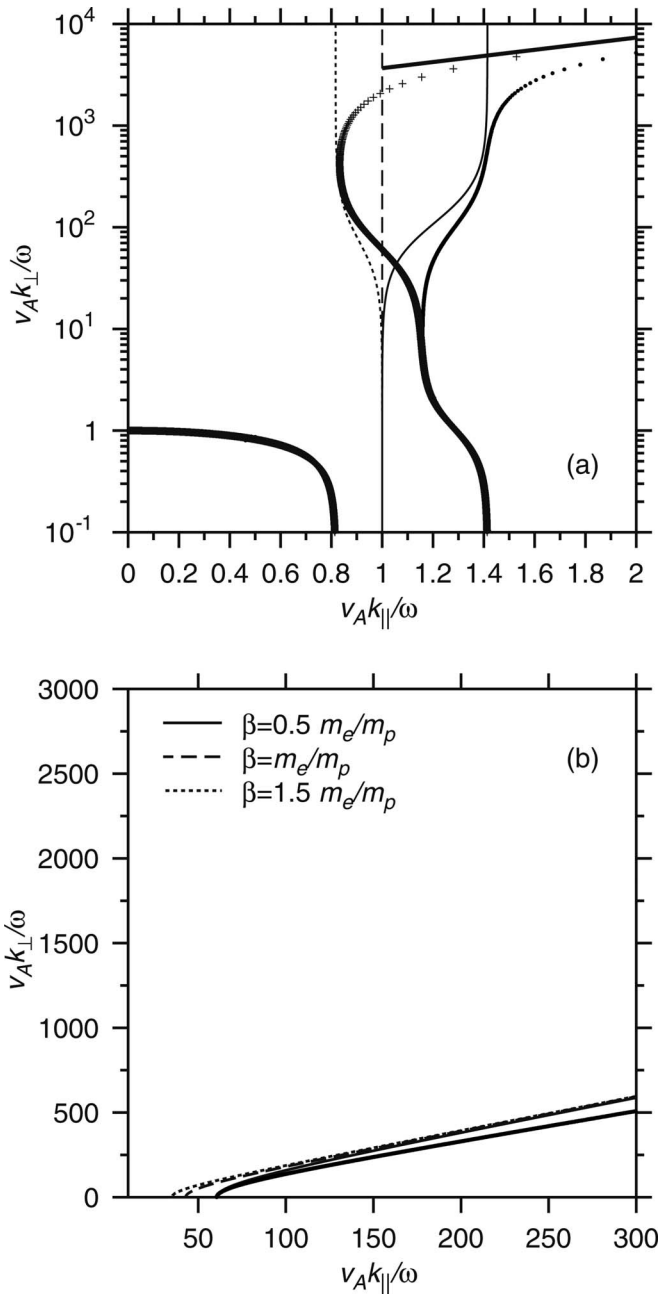

FIG. 8. (a) Same as Fig. 7(a), but for $\omega/\Omega_p=0.5$. The solid black line denotes the resonance cone of the Alfvén branch in the full dispersion relation denoted by $\cos\theta=m_e/m_p(\omega/\Omega_p)(1+m_e/m_p)$. (b) Same as Fig. 7(b), but for $\omega/\Omega_p=0.5$.

$\sqrt{1/\beta}$). Superimposed on the $\beta=\frac{1}{2}m_e/m_p$ case is the solution of the full dispersion relation Eq. (15) (dots) indicating good agreement everywhere.

Figure 8(a) displays results for $\omega/\Omega_p=0.5$ for both the Alfvén and fast modes. The divergence between Eq. (25) and the full dispersion relation [Eq. (15)] is more clearly evident. The previously noted resonance cone is defined by $\cos(\theta)=(m_e/m_p)(\omega/\Omega_p)/(1+m_e/m_p)$ (thick solid line). In addition the whole modified Alfvén branch is displaced to higher values of $v_A k_\parallel/\omega$. The approximate dispersion relation (25) fails in this limit. For the slow mode [Fig. 8(b)] the increase in ω/Ω_p leads to a decrease in the slope [consistent with $\tan^{-1}(\Omega_p/\omega)$].

2. $\beta\sim 1$

Figure 9 displays the numerical solution of the full dispersion relation [Eq. (15)] for $m_e/m_p=1/1836$, $\beta=0.25$, and three values of ω/Ω_p, namely, (a) $\omega/\Omega_p=0.5$, (b) $\omega/\Omega_p=0.7$, and (c) $\omega/\Omega_p=0.9$. An interesting feature is that, as the ratio of ω/Ω_p increases, the Alfvén branch crosses the $k_\parallel$ axis at $1/\sqrt{(m_e/m_p)(\omega^2/\Omega_p^2)-1+(\omega/\Omega_p)}$ and is displaced toward the slow root crossing, which is fixed at $\sqrt{\beta}=v_a/c=2$ (for the present parameters) at which the roots for the two branches "swap," with the slow mode branch now at higher values of $\omega k_z/V_A$ as ω/Ω_p increases.

IV. THE WHISTLER MODE ("ELECTRON MHD")

It is of some interest to see how the nonrelativistic whistler mode follows from the original fluid equations and Faraday's law. In this case we assume that the protons (ions) to be "massive" in the sense that the bulk or proton velocity $\mathbf{u}$, or $\mathbf{u}_p$, is small compared with $\mathbf{u}_e$ so that the current is predominantly carried by the electrons. Ohm's law, Eq. (5), may then be written as

$$\mathbf{E}=\frac{1}{en}\mathbf{j}\times\mathbf{B}_0+\mu_0\lambda_e^2\frac{\partial\mathbf{j}}{\partial t}, \tag{28}$$

where we omitted the electron pressure gradient term, which, in any case, disappears on taking the curl of $\mathbf{E}$. Faraday's law becomes

$$\nabla\times\left(\frac{B_0}{\mu_0 en}\nabla\times\mathbf{B}\times\hat{\mathbf{z}}+\lambda_e^2\frac{\partial}{\partial t}\nabla\times\mathbf{B}\right)=-\frac{\partial\mathbf{B}}{\partial t}, \tag{29}$$

which on expanding yields

$$\frac{\partial}{\partial t}(1-\lambda_e^2\nabla^2)\mathbf{B}=+\frac{V_{Ae}^2}{\Omega_e}\frac{\partial}{\partial z}\nabla\times\mathbf{B}. \tag{30}$$

Taking the curl of this equation yields

$$\frac{\partial}{\partial t}(1-\lambda_e^2\nabla^2)\nabla\times\mathbf{B}=+\frac{V_{Ae}^2}{\Omega_e}\frac{\partial}{\partial z}\nabla^2\mathbf{B}. \tag{31}$$

Eliminating the $\nabla\times\mathbf{B}$ between Eqs. (30) and (31) yields the following wave equation for $\mathbf{B}$:

$$\frac{\partial^2}{\partial t^2}(1-\lambda_e^2\nabla^2)^2\mathbf{B}=-\left(\frac{V_{Ae}^2}{\Omega_e}\right)^2\frac{\partial^2}{\partial z^2}\nabla^2\mathbf{B}. \tag{32}$$

The associated dispersion equation for plane waves of frequency ω and wave vector $\mathbf{k}$ is

$$\omega^2(1+\lambda_e^2k^2)=\pm\frac{V_{Ae}^2}{\Omega_e}k_z k, \tag{33}$$

or

$$k^2=\frac{1}{\lambda_e^2}\frac{\omega}{(\pm\Omega_e\cos\theta-\omega)},$$

where θ is the angle between $\mathbf{k}$ and $B_0\hat{\mathbf{z}}$. The upper sign gives the right handed whistler mode, the dispersion characteristics of which are shown in Fig. 10 as wave normal curves for two frequencies with $\omega/\Omega_p\gtrless 1/2$.

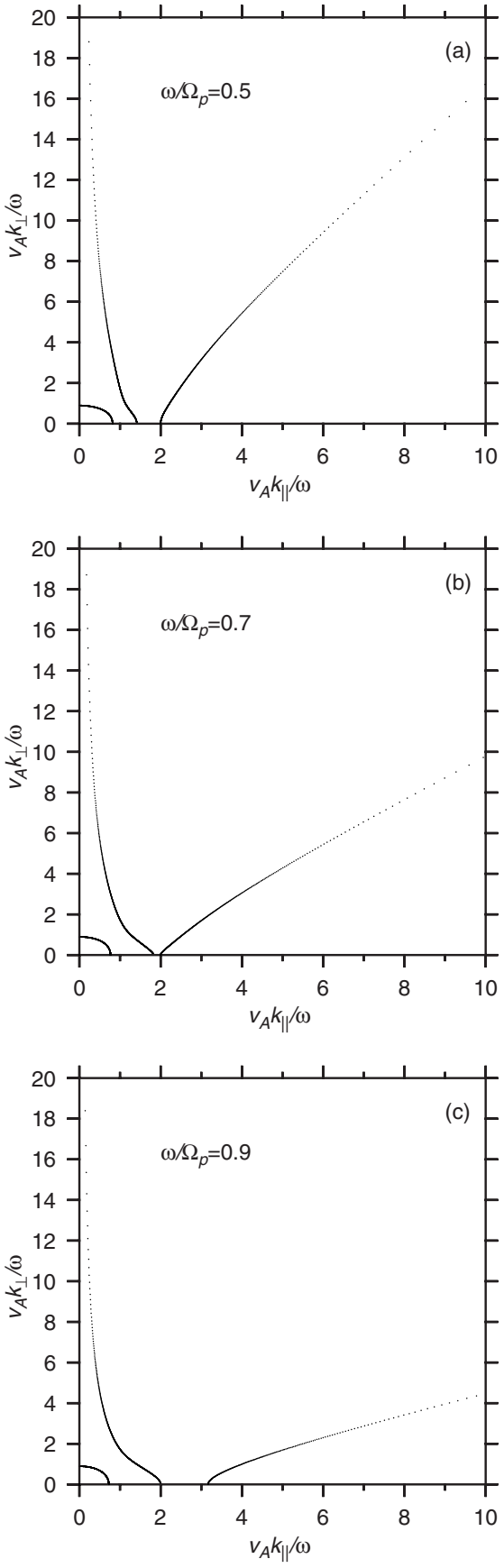

FIG. 9. Solution of full dispersion relation [Eq. (15)] for $m_e/m_p=1/1836$ and $\beta=0.25$ for (a) $\omega/\Omega_p=0.5$, (b) $\omega/\Omega_p=0.7$, and (c) $\omega/\Omega_p=0.9$. The slow mode cuts the $k_\parallel$ axis at v_A/c, while the fast and Alfvén modes cut the axis at $1/\sqrt{(m_e/m_p)(\omega^2/\Omega_p^2)-1+(\omega/\Omega_p)}$ and $1/\sqrt{(m_e/m_p)(\omega^2/\Omega_p^2)-1-(\omega/\Omega_p)}$, respectively. In panel (c) the roots for the slow and Alfvén modes swap.

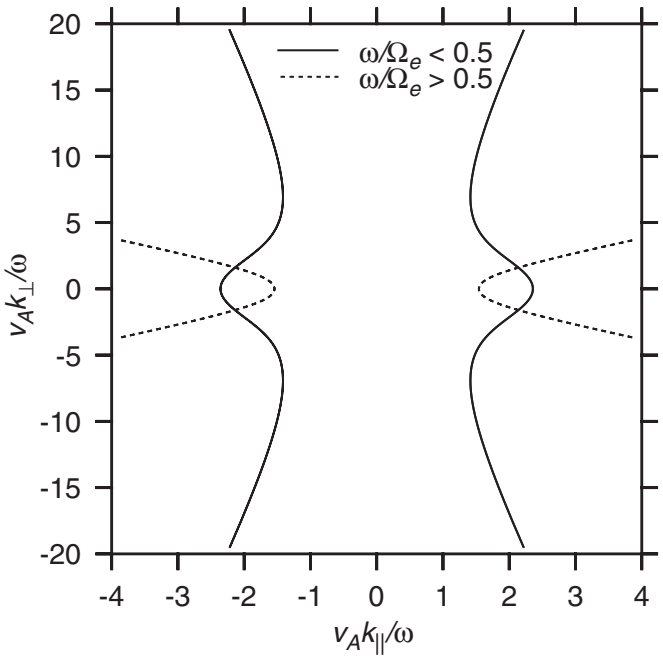

FIG. 10. Plot of $k_\perp$ vs $k_\parallel$ [from Eq. (33)] normalized by ω/V_A for the right handed whistler mode [upper sign in Eq. (33)] for $\omega/\Omega_e<1/2$ (solid line) and $\omega/\Omega_e>1/2$ (dotted line). Specifically, ratio values of $\omega/\Omega_e=0.1$ and $\omega/\Omega_e=0.7$ were used, respectively. Consistent with the rest of the paper, Eq. (33) was reformulated in terms of m_e/m_p and ω/Ω_p and values of $m_e/m_p=0.5$, $\omega/\Omega_p=0.2$, and $\omega/\Omega_p=1.4$ were used $[\omega/\Omega_e=(m_e/m_p)\omega/\Omega_p]$.

V. DISCUSSION

We examined several limits of the full dispersion relation (15), which includes the specific terms in the generalized Ohm's law given by

$$\mathbf{E}=-\mathbf{u}\times\mathbf{B}_0+\frac{1}{en}\mathbf{j}\times\mathbf{B}_0-\frac{\nabla p_e}{en}+\mu_0\lambda_e^2\frac{\partial\mathbf{j}}{\partial t}. \tag{34}$$

Except for the parallel direction (where the Hall term disappears), the order of importance of these individual terms can be assessed as follows. If $\mathbf{E}$ and $\mathbf{u}\times\mathbf{B}_0$ are both regarded as being of order one, then the Hall term $(\mathbf{j}\times\mathbf{B}_0/en)$ is of the order of ω/Ω_p relative to this and the inertial term is of the order of ω/Ω_e relative to the Hall. Therefore the general progression of importance of including terms increases from right to left on the right hand side and the electron inertia term only comes to dominate over the Hall term for higher frequencies of the order of or greater than the lower hybrid frequency. This analysis does not include the pressure term, which must be judged independently for the given set of parameters.

We presented the results in terms of $\mathbf{k}$ diagrams, which is complementary to, but different from the standard presentation (as in Ref. 1), and as such provides further insight. Moreover we graphically illustrated how the limiting solutions contrast with the numerical solution of the full dispersion relation. This comparison is invaluable since it is extremely difficult to interpret how the solutions might diverge from the full dispersion relation based on the initial assumptions alone.

We analyzed in detail the effect of including the various terms on the FLR as defined by Ref. 4. The addition of the Hall term breaks the degenerate solution of the Alfvén branch in the cold plasma limit. For a driven system this would most likely imply that the resonance would form at one field line for small $k_\perp$ but then the resonance position would shift toward an asymptote as $k_\perp \to \infty$. This interpretation is also true with the additional inclusion of electron inertial and finite Larmor radius effects, but the position of the asymptote is now shifted to a position defined by the thermal speed ($k_z = \omega / v_{th}$) rather than the Alfvén speed. For very large values of $\omega k_\perp / V_A$, Hall effects transform this asymptote into a resonance cone. This coupling to the whistler mode would lead to a significant propagation of energy across field lines away from the "original" resonant layer.

Of the three MHD waves branches (fast, slow, Alfvén) the fast magnetoacoustic mode is least effected by the inclusion of the Hall term, but like the Alfvén branch, the slow mode also undergoes substantial modification in this limit. An interesting feature of this analysis is what appears to be a "swapping" of the root behavior along $V_A k_\perp / \omega = 0$ between the Alfvén and slow mode branches (Fig. 9).

APPENDIX: DERIVATION OF WAVE EQUATIONS

The wave Eqs. (12) and (13) of the text are most conveniently derived using the Lighthill variables[13] for the fluid, namely,

$$\triangle \equiv \nabla \cdot \mathbf{u}, \quad \Gamma = \partial u_z / \partial z, \quad w = (\nabla \times \mathbf{u})_\parallel. \tag{A1}$$

Take $\partial / \partial t$ of the divergence of Eq. (2) and use Eq. (3) to give

$$\frac{\partial^2 \triangle}{\partial t^2} - c^2 \nabla^2 \triangle = - \frac{B_0}{\rho_0 \mu_0} \nabla^2 \left(\frac{\partial B_z}{\partial t} \right). \tag{A2}$$

Similarly $\partial / \partial t$ of $\partial / \partial z$ of the parallel component of Eq. (2) yields

$$\frac{\partial^2 \Gamma}{\partial t^2} = c^2 \frac{\partial^2 \triangle}{\partial z^2}. \tag{A3}$$

The parallel component of the curl of Eq. (2) becomes

$$\frac{\partial w}{\partial t} = \frac{B_0}{\rho_0} \frac{\partial j_\parallel}{\partial z}, \quad j_\parallel = (\nabla \times \mathbf{B})_\parallel / \mu_0. \tag{A4}$$

Eliminate the electric field in Faraday's law (4) using Ohm's law (5) to yield

$$\frac{\partial}{\partial t}(1 - \lambda_e^2 \nabla^2) \mathbf{B} = B_0 \frac{\partial}{\partial z} \left(\mathbf{u} - \frac{\mathbf{j}}{en} \right) - B_0 \nabla \cdot \mathbf{u} \hat{z}, \tag{A5}$$

the parallel component of which is

$$\frac{\partial}{\partial t}(1 - \lambda_e^2 \nabla^2) B_z = B_0 (\Gamma - \triangle) - \frac{B_0}{en} \frac{\partial j_\parallel}{\partial z}. \tag{A6}$$

The parallel component of the curl of Eq. (A5) gives

$$\frac{\partial}{\partial t}(1 - \lambda_e^2 \nabla^2) \mu_0 j_\parallel = B_0 \frac{\partial w}{\partial z} + \frac{B_0}{en \mu_0} \frac{\partial}{\partial z} \nabla^2 B_z. \tag{A7}$$

Eliminate the parallel vorticity w in Eq. (A7) using Eq. (A4) to obtain Eq. (12) of the text. Similarly eliminate Γ and Δ from Eq. (A6) using Eqs. (A2) and (A3) to obtain Eq. (13) of the text. The coupled Eqs. (12) and (13) for $j_\parallel$ (Alfvén mode) and B_z (magnetoacoustic modes) yield the wave Eq. (14), which describes the modifications to these modes introduced by the combined effects of Hall currents and electron inertia.

[1] N. F. Cramer, *Physics of Alfvén Waves* (Wiley, Berlin, 2001).
[2] C. K. Goertz and R. W. Boswell, J. Geophys. Res. **84**, 7239, DOI: 10.1029/JA084iA12p07239 (1979).
[3] A. Hasegawa, J. Geophys. Res. **81**, 5083, DOI: 10.1029/JA081i028p05083 (1976).
[4] D. J. Southwood, Planet. Space Sci. **22**, 483 (1974).
[5] W. Press, S. Teukolsky, W. Vetterling, and B. Flannery, in *Fortran*, 2nd ed. (Cambridge University Press, Cambridge, 1992).
[6] C. Q. Wei, J. C. Samson, R. Rankin, and P. Prycz, J. Geophys. Res. **99**, 11265, DOI: 10.1029/94JA00582 (1994).
[7] J. Adlam and J. Allen, Philos. Mag. **3**, 448 (1958).
[8] V. I. Karpman, *Nonlinear Waves in Dispersive Media* (Pergamon, Oxford, 1975).
[9] J. F. McKenzie, E. Dubinin, and K. Saur, J. Plasma Phys. **65**, 213 (2001).
[10] R. Lysak and W. Lotko, J. Geophys. Res. **101**, 5085, DOI: 10.1029/95JA03712 (1996).
[11] A. Streltsov and W. Lotko, J. Geophys. Res. **100**, 19457, DOI: 10.1029/95JA01553 (1995).
[12] A. Streltsov and W. Lotko, J. Geophys. Res. **101**, 5343, DOI: 10.1029/95JA03762 (1996).
[13] M. Lighthill, Philos. Trans. R. Soc. London, Ser. A **252**, 397 (1960).